Heliyon 10 (2024) e34841

Contents lists available at ScienceDirect

Heliyon

journal homepage: www.cell.com/heliyon

Research article

Chemometrically-aided general approach to novel adsorbents studies: Case study on the adsorption of pharmaceuticals by the carbonized *Ailanthus altissima* leaves

Jevrem Stojanović [a], Maja Milojević-Rakić [b], Danica Bajuk-Bogdanović [b], Dragana Ranđelović [c], Miroslav Sokić [c], Biljana Otašević [a], Anđelija Malenović [a], Aleksandra Janošević Ležaić [d], Ana Protić [a,*]

[a] *Department of Drug Analysis, University of Belgrade-Faculty of Pharmacy, Vojvode Stepe 450, 11000 Belgrade, Serbia*
[b] *University of Belgrade-Faculty of Physical Chemistry, Studentski trg 12-16, 11158 Belgrade, Serbia*
[c] *Sector for metallurgical technology and environmental protection, Institute for Technology of Nuclear and Other Mineral Raw Materials, Bulevar Franš d'Eperea 86, 11000 Belgrade, Serbia*
[d] *Department of Physical Chemistry and Instrumental Methods, University of Belgrade-Faculty of Pharmacy, Vojvode Stepe 450, 11000 Belgrade, Serbia*

ARTICLE INFO

Keywords:
Adsorption
Biochar
Invasive plant
Pharmaceuticals
Experimental design

ABSTRACT

A chemometrically based approach was applied to select the most efficient drug adsorbent among the biochars obtained from the novel feedstock, the leaves of the invasive plant (*Ailanthus altissima*). The representative target adsorbates (atenolol, paracetamol, ketorolac and tetracycline) were selected on the basis of their physicochemical properties to cover a wide chemical space, which is the usual analytical challenge. Their adsorption was investigated using design of experiments as a comprehensive approach to optimise the performance of the adsorption system, rationalise the procedure and overcome common drawbacks. Among the response surface designs, the central composite design was selected as it allows the identification of important experimental factors (solid-to-liquid ratio, pH, ionic strength) and their interactions, and allows the selection of optimal experimental conditions to maximise adsorption performance. The biochars were prepared by pyrolysis at 500 °C and 800 °C (BC-500 and BC-800) and the $ZnCl_2$-activated biochars were prepared at 650 °C and 800 °C (AcBC-650 and AcBC-800). The FTIR spectra revealed that increasing the pyrolysis temperature without activator decreases the intensity of all bands, while activation preserves functional groups, as evidenced by the spectra of AcBC-650 and AcBC-800. High temperatures during activation promoted the development of an efficient surface area, with the maximum observed for AcBC-800 reaching 347 $m^2\ g^{-1}$. AcBC-800 was found to be the most efficient adsorbent with removal efficiencies of 34.1, 51.3, 55.9 and 38.2 % for atenolol, paracetamol, ketorolac and tetracycline, respectively. The models describing the relationship between the removal efficiency of AcBC-800 and the experimental factors

Abbreviations: BCs, Biochars; AcBCs, Activated Biochars; DoE, Design of Experiments; OFAT, One-Factor-At-A-Time; HPLC, High-Performance Liquid Chromatography; CCD, Central Composite Design.

* Corresponding author.
E-mail addresses: jstojanovic@pharmacy.bg.ac.rs (J. Stojanović), maja@ffh.bg.ac.rs (M. Milojević-Rakić), danabb@ffh.bg.ac.rs (D. Bajuk-Bogdanović), d.randjelovic@itnms.ac.rs (D. Ranđelović), m.sokic@itnms.ac.rs (M. Sokić), biljana.otasevic@pharmacy.bg.ac.rs (B. Otašević), andjelija.malenovic@pharmacy.bg.ac.rs (A. Malenović), aleksandra.janosevic@pharmacy.bg.ac.rs (A.J. Ležaić), anna@pharmacy.bg.ac.rs (A. Protić).

https://doi.org/10.1016/j.heliyon.2024.e34841
Received 20 April 2024; Received in revised form 16 July 2024; Accepted 17 July 2024
Available online 18 July 2024

studied, showed satisfactory predictive ability (predicted $R^2 > 0.8$) and no significant lack-of-fit was observed. The results obtained, including the mathematical models, the properties of the adsorbates and the adsorbents, clearly indicate that the adsorption mechanisms of activated biochars are mainly based on hydrophobic interactions, pore filling and hydrogen bonding.

1. Introduction

Liquid phase adsorption is, indisputably, one of the leading solutions for a number of processes, including catalysis, advanced treatment of wastewater, sample preparation, and chromatographic analysis in analytical laboratories. In the search for sustainable solutions, the carbonization of low-cost, widely available and currently unused biomass has attracted particular interest in recent years. Carbonaceous materials obtained by the carbonization of biomass are also known as biochars (BCs) [1,2]. When physical or chemical activation processes are used to improve the properties of BCs, the resulting solid products are sometimes referred to as activated biochars (AcBCs) [3–5], although due to inconsistencies in the literature, the terms biochars or activated carbons are interchangeably used to refer to these materials. It is believed that BCs and AcBCs can overcome the disadvantages of some currently used commercially available adsorbents such as the consumption of non-renewable raw materials, high energy costs, production costs and difficult regeneration [6,7]. In sorbent-based sample preparation techniques, these carbonaceous adsorbents can be advantageous due to their chemical stability at extreme pH values, the structural properties that allow them to interact with organic molecules, and finally their low cost and reduced negative impact on the environment [8]. A variety of biomasses have been tested as raw materials for the production of BC, including agricultural and forestry residues, sewage sludge, food waste and so on [9,10]. In terms of feedstock selection, *Ailanthus altissima* emerges as a promising choice due to its invasive nature, widespread distribution and allelopathic effect, thereby contributing to remarkable negative impacts on biodiversity and the ecosystem [11,12]. Complete eradication of this plant is currently impossible. For this reason, its use in the production of adsorbents could be a successful attempt to increase its value and use more environmentally friendly materials from renewable sources. To the best of our knowledge, such a possibility of using *A. altissima* has not yet been tested.

The adsorption process is rather complex as it depends on the properties of the adsorbent, the adsorbate and the experimental conditions. It is known that the properties of biochar vary depending on the feedstock used and the conditions set during carbonization. For single biomass, it is advisable to prepare and test several adsorbents by altering carbonization conditions (temperature, impregnation with chemicals) to explore its full potential for use as a feedstock. The proper investigation of the adsorption process requires an adequate selection of representative adsorbates. Drug molecules as target adsorbates cover a wide chemical space in terms of their molecular properties such as polarity, pKa, lipophilicity, size, etc. These properties determine the ability of the drug molecules to form different types of interactions (ionic, dispersion interactions, hydrogen bonding, etc.) with the surface of the adsorbent. Therefore, the adsorbate model substances should be selected to fairly represent the actual analytical problem and cover the wide chemical space. However, it is necessary to limit the number of model substances during the preliminary study, which only aims to identify the adsorbent with the desired performances, in order to carry out this step quickly, with minimum experimental effort, associated material consumption and costs.

The experimental conditions under which the adsorption takes place can influence both its rate and degree. The influence of various experimental factors, such as temperature, solid-to-liquid ratio, pH and ionic strength of the solution, has often been shown to be significant in the literature [13–18]. When it comes to comparing the efficiency of different adsorbents, the question arises as to which experimental conditions should be selected. To answer this question, we must first understand how experimental factors influence adsorption. Gaining such an understanding of the system by adjusting one factor at a time would not only lead to a high number of experiments, but also to a high consumption of adsorbents, increased energy consumption for the preparation of new quantities of adsorbents, increased chemical consumption and, above all, to wrong conclusions regarding the optimal adsorption conditions. This problem is even more pronounced when the production of carbonaceous material takes place at high temperatures, which normally leads to a significantly lower yield. On the other hand, while it is easy to subject all adsorbents to identical conditions, the variability or adaptability of experimental conditions that may occur in real-life applications is not captured. Ultimately, these two approaches can lead to an incorrect selection of the optimal adsorbent among the tested materials.

To address this problem, Design of Experiments (DoE) can be used as it stands out as a highly efficient statistical approach that allows a comprehensive exploration of systems influenced by multiple factors while minimising the number of experiments required [19,20]. In contrast to the One-Factor-At-A-Time (OFAT) approach commonly used in adsorption studies [21–27], DoE offers several notable advantages that have contributed to its widespread adoption in recent years. One of the main advantages is the ability to identify significant interactions between factors while minimising the number of experiments required. The OFAT study of experimental factors, in which a single factor is examined at certain levels and then another factor is examined at fixed levels of the previous factor, may require a similar number of experiments as the DoE approach. However, OFAT excludes many possible combinations of factor levels and therefore cannot identify interactions between factors or guarantee that the optimal conditions discovered are globally optimal [28]. In the OFAT approach, the researcher decides how many levels of which factors should be examined, which can lead to an unnecessarily large number of experiments, in addition to the disadvantages of OFAT already mentioned. These advantageous features of DoE are facilitated by a well-structured experimental plan that allows for the simultaneous and systematic variation of multiple factors. Since DoE takes into account possible interactions between the investigated factors as well as the possibility of curvilinear relationships between the response and the factors, it is a much more reliable way to find a global optimum, i.e. truly

optimal conditions, compared to the OFAT approach. Moreover, a particularly useful trait of DoE is the empirical polynomial model obtained as a result of the procedure. This model relates the response of the system to the factors under investigation and can therefore be used to predict the response values based on the values of the factors in the defined factor range. In some situations, where adjustments to factor values are required, such empirical models prove invaluable as they provide the flexibility to choose alternative factor values that maintain the desired system performance. The values of the model coefficients reflect the nature and magnitude of the effects of the factors investigated. Empirical models thus serve as a basis for gaining knowledge about the system behaviour within the explored experiment space. As long as the model is valid, accurate predictions of the response can be made for any point within the experiment space [29]. Although it is clear that these advantages could be utilised in the study of novel adsorbents, only a few papers dealing with drug adsorption have applied DoE to date [14–17,30,31].

This research introduces a chemometrically based, widely applicable framework for the selection of drug adsorbents with the highest removal efficiency. The main objective of this research is to propose the selection of adsorbates with strategically selected model substances (adsorbates) whose physicochemical properties adequately cover the chemical space of the adsorbates of interest. In this way, the conclusions regarding the most efficient adsorbent can be applied generally and not only for a few selected adsorbates. It should be emphasised that the method presented here differs significantly from the approaches used to study novel adsorbents obtained from biomass [32–34], where one or a small number of adsorbates are usually selected without well-defined criteria. In addition, adsorption tests are carried out using the DoE methodology to investigate the experimental conditions at which the removal efficiency reaches its maximum. In this way, the mathematical models are obtained. They can describe the influence of the experimental conditions on the adsorption, enable an insight into the whole adsorption system, identify the optimal adsorption conditions, the interaction of the experimental factors and give an indication of the underlying interactions between adsorbate and adsorbent. In addition, this approach can ensure the lowest possible material consumption, which is highly desirable when investigating biochars.

At the end, it can be decided which adsorbents need to be subjected to a detailed physicochemical characterissation. The adsorbents for which further tests are not fruitful, due to their limited applicability for a narrow range of adsorbates or adsorption conditions or because they do not perform sufficiently well over the entire experimental domain studied. This offers the opportunity to reduce the cost, time and effort involved in testing adsorbents.

The aforementioned potentials of the chemometrically-aided framework are tested in the case study on the adsorption of four model adsorbates (atenolol, paracetamol, ketorolac and tetracycline) on carbonaceous materials derived from *A. altissima* (four differently prepared adsorbents). The specific surface area determined by BET and the characteristic functional groups determined by FTIR analysis, were also presented to ensure the plausibility of the proposed adsorption mechanisms.

2. Materials and methods

2.1. Biochar and activated carbon preparation

The leaves of *A. altissima* before the carbonization process, were washed with tap water and then with distilled water, then dried for two weeks at room temperature to a constant mass and then crushed (grounded) in a mill (particle size <0.2 mm). The resulting powdery material was stored in a desiccator at room temperature prior to its carbonization.

The carbonization of the powdered leaves of *A. altissima* was carried out by pyrolysis in a muffle furnace under an argon atmosphere. The first carbonization was carried out at 500 °C for 2h to produce BC-500. Pyrolysis of BC-500 for another 2h at 800 °C was carried out to produce BC-800. To produce activated carbon, BC-500 was first impregnated with $ZnCl_2$ in a mass ratio of 3:1. Pyrolysis of the impregnated BC-500 was carried out at 650 °C for 2h to produce AcBC-650 and at 800 °C for 2h to produce AcBC-800. The argon flow rate was 60 mL min^{-1}, while the heating rate was 10 °C min^{-1}.

2.2. Chemicals and reagents

The reference standard substances used in this study were atenolol (>99 %), paracetamol (>99.9 %), ketorolac tromethamine (>98.5 %), and tetracycline hydrochloride (>99 %), obtained from Sigma Aldrich Chemie GmbH (Taufkirchen, Germany). All standard solutions and HPLC eluents were prepared from HPLC-grade water produced by Adrona CB -1905 (Adrona SIA, Riga, Latvia). The hydrochloric acid (37 %, p.a.) was obtained from Sigma Aldrich Chemie GmbH (Taufkirchen, Germany), potassium hydroxide pellets (p.a.) from Merck KGaA (Darmstadt, Germany), and potassium chloride (p.a.) from Carl Roth GmbH + Co KG (Karlsruhe, Germany). Acetonitrile (HPLC gradient grade) used for eluent preparation was purchased from Sigma Aldrich Chemie GmbH (Taufkirchen, Germany). Perchloric acid (70 % p.a., Riedel-de Haën AG, Seelze, Germany), was used as the mobile phase additive. Formic acid (p.a., Sigma Aldrich Chemie GmbH, Taufkirchen, Germany) and ammonium formate (p.a., Honeywell International Inc., Muskegon, Michigan) were used to prepare the buffered eluent. Zinc chloride (p.a.) used during preparation of AcBCs was purchased from Merck (Darmstadt, Germany).

2.3. Preparation of reference standard solutions

Stock solutions of reference standard substances were prepared at a concentration of 1 mg mL^{-1}. Adsorption test working solutions, set at a 50 μg mL^{-1} concentration, were prepared from a stock solution. To ensure an ionic strength adjustment, 3 M KCl was added, followed by dilution with water. The pH value of each working solution was adjusted with 10 M/1 M potassium hydroxide or concentrated (37 %)/1 M HCl using a pH meter Meterlab PHM210 (Radiometer analytical, Villeurbanne, France). Appropriate

volumes of stock solutions were diluted with water to prepare calibration solutions.

2.4. Batch adsorption experiments

The adsorption experiments were performed in batch mode by suspending the appropriate mass of adsorbent in the solution containing a single adsorbate. Initial concentration of adsorbates, temperature and shaking speed were 50 μg mL^{-1}, 23 °C and 500 rpm for all batch adsorption experiments. Digital Vortex-Genie 2 (Scientific Industries, Bohemia, New York) was used to agitate the samples to ensure proper contact of the adsorbents with the solution. During the optimisation procedure, samples were shaken for 60 min. After the appropriate shaking time, the samples were centrifuged using DragonLab D2012 Plus (DLAB Scientific Co., Ltd., Beijing, China) centrifuge. The residual concentration of adsorbates in the supernatant was determined by the HPLC methods described below. Based on the residual concentration of the adsorbate after 60 min (C_t), the removal efficiency (R (%)) and adsorbed amount (q_t) for the given initial concentration of adsorbate (C_i) were calculated as follows:

$$R(\%) = \frac{(C_i - C_t)}{C_i} \times 100 \quad (1)$$

$$q_t = \frac{(C_i - C_t) \times V}{M} \quad (2)$$

where V is the volume of solution and M is the mass of adsorbent. Control samples were used to check for possible causes of concentration changes other than adsorption, such as solute degradation or precipitation. The blank test was performed similarly, without adsorbent present.

2.5. Design of experiments (DoE)

The study of the influence of selected experimental factors on the adsorption of model substances and the search for optimal conditions for further studies were carried out using the central composite design (CCD) [35]. The search for optimal experimental conditions is also necessary to determine the values of the experimental factors under which the efficiency of different adsorbents should be compared. The CCD usually consists of a full factorial design with 2^k points, a star design with $2k$ points and a central point with a certain number of replicates, where k is the number of factors [36]. While factorial points are sufficient to estimate the linear model terms and interactions, the axial point provides the possibility to estimate quadratic terms and center points allow the estimation of the pure experimental error and stabilise the variance of the model predictions [35]. The above properties make CCD a suitable design for optimisation. In addition, the position of the axial points influences the rotatability of the design. Rotatable designs are desirable as this ensures that the variance of the prediction is the same for each of the equidistant points, regardless of their direction in the experimental space under study. However, to achieve the rotatability of the experimental design containing a large number of experimental factors, the axial points must be further away from the centre of the experiment space, which may lead to a loss of significant information near the centre of the space [35]. We decided to investigate factors whose changes are likely to lead to a change in adsorption mechanisms and/or a significant change in removal efficiency. Since our study included three factors, the rotatable CCD was deemed suitable for optimisation.

To optimise the removal efficiency of the adsorption process, the experiments were performed by varying the pH, ionic strength and solid-to-liquid ratio in the ranges 3–12, 30–300 mM and 0.1–0.4 mg mL^{-1}, respectively. The limits of the ranges given above are used as values for the axial points. The CCD experiments with the corresponding levels of the investigated factors are shown in Table S1 in standard order. The upper pH limit for the adsorption of tetracycline was lowered to 10 to avoid a high rate of drug degradation. Three additional replicates were performed in the central point of the experiment space and the total number of experiments was 18. This corresponds to the usual recommendation to carry out three to five experiments in the central point [36]. Experiments were performed in a completely randomised order. Optimisation was performed with respect to one response – the removal efficiency (R (%)).

2.6. High-performance liquid chromatography (HPLC) methods for analysis of samples from batch adsorption experiments and control samples

The HPLC instrument used in this study was Finnigan Surveyor Thermo Scientific (Thermo Fisher Scientific, Waltham, Massachusetts, USA), equipped with LC Pump Plus, Autosampler Plus, UV-VIS Detector Plus. Analysis of all samples was performed on Agilent Technologies Zorbax Eclipse XDB-C18 column (4.6 × 150 mm, 5 μm) with a mobile phase flow rate of 1 mL min^{-1} and column temperature of 30 °C. Further details on the HPLC methods used can be found in Table S2. The concentrations of the analytes were calculated against the calibration curves given in Table S3.

2.7. Physicochemical characterisation of adsorbents

The point of zero charge (pH_{pzc}) of *A. altissima* leaf BCs and AcBCs was determined from aqueous suspensions of the tested samples: 5 mg of the sample was weighed and suspended in 50 mL of 0.01 M KNO_3 solution (according to the method described by Milonjić et al., 1975 [37]) and then left in an ultrasonic bath for 3 min. The initial pH values of the suspension were adjusted with HNO_3 and

KOH to a value between 2.0 and 9.0. The zeta potential of the studied BCs and AcBCs was determined using the Zetasizer Nano Z instrument (Malvern, U.K.).

FTIR spectra of the samples were recorded using a Nicolet iS20 FTIR Spectrometer (Thermo Scientific, USA) in the wavenumber range 4000-400 cm^{-1}. The resolution was set to 4 cm^{-1} and 32 scans per spectrum were averaged. Potassium bromide pellet technique was used for sample preparation.

An analysis of the specific surface area and pore parameters (volume and size) was conducted using the Brunauer–Emmett–Teller (BET). This analysis was performed utilising the ASAP 2020 system (Micromeritics, USA). Prior to measurements, the samples were subjected to degassing under a vacuum at a temperature of 150 °C for a duration of 10 h.

2.8. Correlation analysis

To discern potential interactions between AcBC-800 and the tested drug molecules, analysis of correlations between the appropriate adsorption system response (adsorbed amount), molecular descriptors and experimental factors was conducted. This involved merging removal efficiency, adsorbed amount, pH, ionic strength, and solid-to-liquid ratio data from four CCD procedures into a single dataset. Additionally, the molecular properties were calculated using MarvinSketch 22.22 for each pH value and included in a dataset. The total charge of the ionised molecules was determined by calculating the sum of the products of absolute charges and the abundance of specific ionisation states at different pH values, allowing a comprehensive representation of the net charge under different conditions. In this way, a dataset with a total of 72 instances was obtained.

2.9. Software

The DoE methodology was implemented using Design-Expert 7.0.0 software (Stat-Ease, Inc., Minneapolis, USA). The molecular properties of the model substances were calculated using MarvinSketch 22.22. (Chem Axon Ltd., Budapest, Hungary). The analysis of correlations between experimental factors, molecular properties, and the removal efficiency was carried out using the *pandas* module and data visualisation using *matplotlib* and *seaborn* libraries in Python version 3.11.5.

3. Results

3.1. Physicochemical characterisation of adsorbents

The zeta potential was measured to take into account the changes in the properties of the adsorbent depending on the experimental pH conditions. Changes in the ionisation of surface functional groups with the change of the solution pH lead to a change in the net charge of the adsorbent surface, which consequently affects the affinity of the adsorbent to charged solutes. Zeta potential values are given in Fig. 1. The higher extent of colloid surface negative charge is rising with acidity decrease for all samples, as expected for biochar samples [38].

In this study, low values of the specific surface area of non-activated biochar were determined using the BET method (S_{BET}), namely 4.0 $m^2\ g^{-1}$ and 0.8 $m^2\ g^{-1}$ for BC-500 and BC-800, respectively. For activated biochar determined S_{BET} is 93.4 $m^2\ g^{-1}$ for AcBC-650, and 346.6 $m^2\ g^{-1}$ for AcBC-800, confirming the hypothesis that it is important to ensure a high temperature during activation with $ZnCl_2$ in order to achieve an efficient increase in surface area, which is important for satisfactory adsorption performance.

The FTIR spectra of the samples are shown in Fig. 2, in two regions 4000-2500 cm^{-1} (a) and 2000-400 cm^{-1} (b). It was found that only in the presence of $ZnCl_2$ the surface functional groups of the precursor biochar (BC-500) are preserved during its carbonization. In the spectrum of the carbonized sample BC-800, obtained in the absence of $ZnCl_2$ activator, the characteristic bands of functional groups

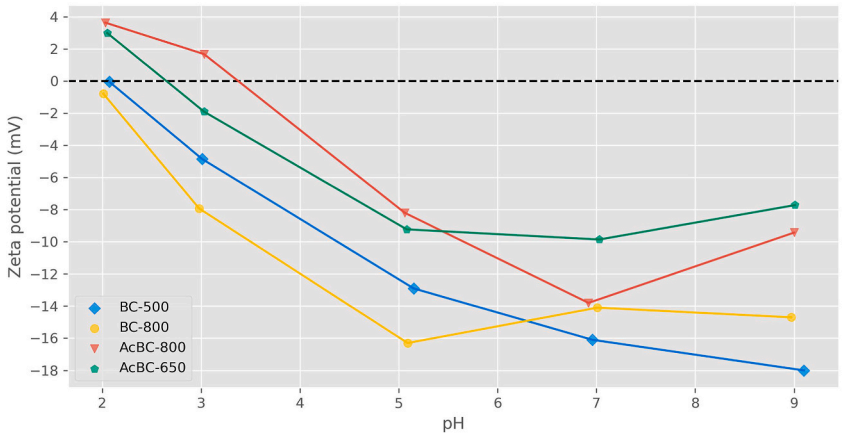

Fig. 1. Zeta potential (mV) values of BC-500, BC-800, AcBC-650 and AcBC-800 as a function of pH.

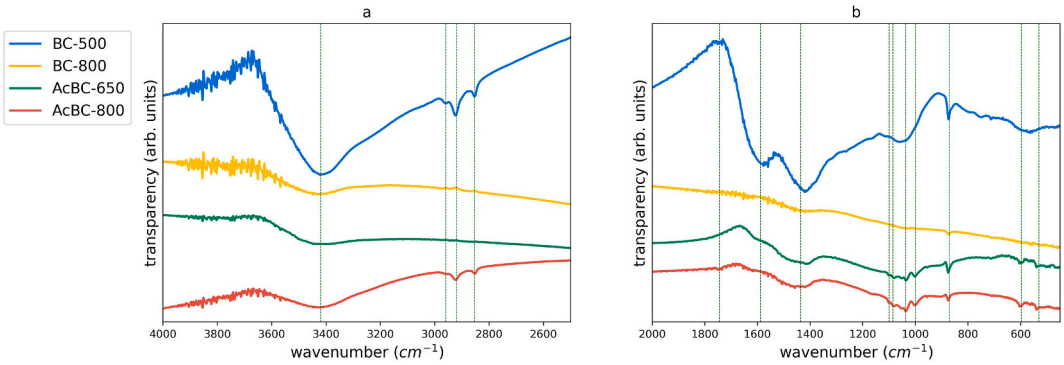

Fig. 2. FTIR spectra of BC-500, BC-800, AcBC-650 and AcBC-800 in wavenumber range: a) 4000-2500 cm^{-1}; and b) 2000-500 cm^{-1}.

are not visible.

All observed bands in the AcBC samples are of lower intensity than in the spectrum of BC-500, as expected since the carbonization temperature is inversely proportional to the amount of surface functional groups in biochar [39]. In the first region (Fig. 2a), the broad band at 3420 cm^{-1} corresponds to the O–H stretching observed in all samples' spectra [40,41]. The bands at 2920 cm^{-1} and 2853 cm^{-1} likely originate from the asymmetric and symmetric stretching of methylene groups, respectively [42]. In the second region (Fig. 2b), very weak signal at 1720 cm-1 could indicate carbonyl-containing groups such as ketones, carboxylic acids, and their derivatives [43]. The bands at 1589 cm^{-1} and 1436 cm^{-1} can be attributed to C═C stretching of aromatic rings [42,44]. However, according to literature [43], these bands could be due to the stretching of carboxylates. It is therefore possible that some of the carboxyl groups have formed salts with the Zn^{2+} ions during the activation process. However, since the intensity of the band at 1589 cm^{-1} is not higher than that of the band at 1436 cm^{-1}, as expected for carboxylates [43], it appears that both aromaticity and carboxylates have contributed to the band intensities. It is also possible that C–OH deformation (in-plane bending) was involved in the formation of the band at 1436 cm-1, which is further evidence for the presence of alcohols/phenols [43]. The region characteristic of C–O stretching is complex. Four bands at 1100, 1085, 1037, and 1000 cm^{-1} could be assigned to asymmetric C–C–O stretching of secondary/tertiary alcohols, asymmetric C–O–C stretching of ethers, asymmetric C–C–O stretching of primary alcohols and symmetric C–C–O stretching of tertiary alcohols, respectively [42–44]. Therefore, it is likely that both alcohol and ether groups are present on the surface of AcBC-800. The band at 872 cm^{-1} could also indicate the presence of alcohols and ethers, as it could have resulted from the symmetric stretching of alcohol or ether groups [42]. Another possible contribution to this band could appear from out-of-plane C–H vibrations of aromatic rings [43]. Near the bottom of the region, the bands observed at 597 cm-1 and 531 cm-1 are most likely due to vibrations of metal oxides such as ZnO or CaO [45,46].

3.2. Selection of model substances

The model substances were selected based on their different physicochemical properties. Atenolol represents a drug molecule that is predominantly positively charged across a broad pH value range (representative of cationic structures). Similarly, paracetamol exemplifies a neutral drug, ketorolac illustrates anionic (negatively charged in a broad pH range) and tetracycline represents a zwitterionic drug. In addition, the selected model substances cover a relatively wide lipophilicity range under different experimental conditions. Model substances also possess significantly different numbers of proton-donor and proton-acceptor sites as well as polarizability. The structures of the model substances are shown in Fig. S1, while the calculated properties and distribution of ionisation forms over the defined pH range are graphically represented in Fig. S2 and Fig. S3, respectively. The molecular properties shown in Fig. S2 are selected based on their ability to represent the potential for ionic interactions, hydrogen bonding, London dispersion interactions, dipole interactions and pore-filling mechanisms.

3.3. Selection of experimental factors and their ranges to be investigated through DoE

The pH value of the solution is considered important because it can affect both the charge of the solute (Fig. S3) and the surface charge of the adsorbent (Fig. 1), thus changing the intensity of the electrostatic interactions. In addition, the pH of the solution affects the lipophilicity of the solutes (Fig. S2) and therefore probably alters the contribution of the hydrophobic effect to adsorption. The ionic strength of the solution affects ionic interactions and hydrophobic interactions. Theoretically, depending on whether the ionic interactions are attractive or repulsive, salts can increase or decrease the extent of adsorption. For instance, salts can neutralise charges with the same polarity of both the adsorbate and the adsorbent surface, resulting in a reduction of repulsive electrostatic interactions and consequently an increase in adsorption. Alternatively, they can also neutralise charges with opposite polarity, which hinders the attractive electrostatic forces and thus weakens adsorption [47]. In addition, "salting out" is likely to occur at higher salt concentrations, which may enhance hydrophobic interactions between adsorbent and adsorbate [48].

When considering the ranges of experimental factors to be studied, extreme pH values may cause degradation of the drug, which is not desirable, so these pH values were not included in the experiments (Table S1). High ionic strength may lead to precipitation of the

adsorbate due to the "salting out" effect or surface charge neutralisation and reduced thickness of the electric double layer of the suspended adsorbent particles, resulting in their agglomeration and ultimately lower removal efficiency. The dose of adsorbent should be properly optimised to ensure satisfactory removal efficiency. Too small dosage of adsorbent may result in small changes in solute concentrations which would lead to inaccurate calculation of adsorbed amount in the subsequent study [49]. Conversely, too large a solid-to-liquid ratio may result in the aggregation of adsorbent particles and a smaller contact area between adsorbent and solutes.

Factors such as contact time and shaking speed were not investigated. The contact time was kept constant and limited to 60 min in order to select the most efficient sorbent. This was considered important as a rapid adsorption process is desirable for most applications. In some applications, the available contact time is extremely limited and the initial rate is of utmost importance for adsorption efficiency [50]. It is known that the shaking speed influences the mass transfer process when external (film) diffusion is the rate-limiting step. When the shaking speed is high, the liquid film around the particles becomes thin, which enables a fast film diffusion process [51]. Therefore, the shaking speed was kept relatively high (500 rpm) to prevent a significant decrease in the film diffusion rate. The temperature during the adsorption tests was also kept constant, as the kinetics of the degradation reactions can increase when the temperature is increased [52] and it is therefore advisable not to increase the temperature during sorbent-based sample preparation.

3.4. DoE models

ANOVA summary of the models obtained by the DoE approach is given in Table S4. The polynomial order was selected based on the sequential addition of model terms and the resulting statistical significance, lack-of-fit and predictive accuracy of the models. All obtained models were statistically significant ($p < 0.05$), while the lack-of-fit term was not statistically significant in any case ($p > 0.05$). Stepwise multiple linear regression was used to generate the models. All terms with a p-value less than 0.1 were retained in the model. In some cases, the values of the responses were transformed to meet the assumptions of multiple linear regression. No outliers were detected and lack-of-fit was not significant. The models are presented in terms of coded values of the factors in the text below.

Removal efficiency was selected as the most appropriate response of the system for building the model, as it was considered better suited to reflect the changes in the factor levels compared to the other responses. The other often used response in the adsorption systems is the amount of solute adsorbed in time t (q_t). It was considered a less appropriate response when using DoE because it can be spuriously large when the small dose of adsorbent and low decrease in solute concentration are combined with relatively high experimental variability [49]. Furthermore, the variation of q_t can be insignificant if the ratio of adsorbate concentration to adsorbent quantity leads to almost complete coverage of the adsorbent surface. The calculated values of response are shown in Table S5.

3.5. Adsorption of model substances on BC-500 and BC-800

Regardless of the experimental conditions, no significant adsorption of atenolol, paracetamol, and ketorolac was observed on BC-500 and BC-800. Tetracycline was the only substance that showed an affinity for the aforementioned BCs, but the removal efficiency was relatively small in the entire experiment space studied (9.2 % and 11.3 % mean value for BC-500 and BC-800, respectively). The polynomial models describing the influence of the experimental factors on the extent of tetracycline removal from solution by adsorption on BC-500 and BC-800, respectively, are given by the following equations:

$$R(\%) = 11.40 + 3.18 \times A - 0.24B - 2.93 \times B^2 \quad (3)$$

$$sqrt(R(\%)) = 3.77 - 0.95 \times AB + 0.67 \times BC - 0.91 \times B^2 \quad (4)$$

where A stands for the solid-to-liquid ratio and B for the pH of the solution, AB denotes the interaction between the solid-to-liquid ratio and the pH of the solution, and BC signifies the interaction between pH and ionic strength.

However, the models obtained in the case of BC-500 and BC-800 do not fully describe the variation in the observed values of the experimental response, as indicated by the values of the coefficient of determination, shown in Table S4. This could be since the changes in removal efficiency within the studied experiment space are generally small. On the other hand, the variability observed in the replicated experiments under the conditions of the central point of the experimental design is quite large. For example, the removal efficiency in all experiments was between 0.6 % and 17.5 %, while it was between 6.6 % and 11.5 % in the replications at the central point in the case of BC-500. The rather high variability of the response in the repeated experiments under the same conditions could be due to the heterogeneity and random distribution of the adsorption sites of the BCs. The distribution of the adsorption sites cannot be controlled as it probably originates from the natural starting material [53]. Since the starting material is the leaf of *A. altissima*, which is available almost all year round and the plant can grow on different soil types, seasonal and geographical variations likely lead to differences in the chemical composition of the leaves and consequently to even greater variations in the adsorption capacity of the resulting BCs. Consequently, further drug adsorption studies with these materials could be laborious, require a high number of replicates, require a high material consumption or even be impossible. Although the use of the obtained models to define optimal experimental conditions is limited because of the low adjusted and predicted R^2 values, performed DoE optimissation at the beginning of the research demonstrated the low reproducibility of the experiments, low removal in the entire experiment space and encouraged researchers to focus on the other potentially suitable adsorbents. While the traditional adsorption tests usually involve replicates of each experiment to distinguish between the true effects and the random variations of the response, the DoE approach allowed the estimation of the experimental error by only four experiments. Moreover, as can be seen from Eq. (4), some factor interactions were

also successfully revealed, which also supports the chosen research strategy.

From the magnitude of the model coefficients in Eq. (3) it can be seen that the ionic strength of the solution played no role in the adsorption of tetracycline on BC-500, the dosage of the adsorbent was of minor importance, while the pH of the solution was of major importance. None of the interactions studied were significant. The plot showing the dependence of the observed response on the solid-to-liquid ratio and the pH is shown in Fig. 3, while the plots of main effects are given in Fig. S4. It can be seen that an increase in the solid-to-liquid ratio leads to an increase in the extent of removal of tetracycline, while the extent of removal shows a downward parabolic dependence on pH, with the highest removal at pH around 6.5. Thus, a higher dosage of adsorbent did not result in agglomeration of adsorbent particles and consequent lower removal efficiency. It is possible that the pH value of 6.5 is the environment that favors attractive ionic interactions since tetracycline is in the form of a zwitterion (Fig. S3) and the surface charge of the adsorbent is near its minimum (Fig. 1). A similar relationship between the removal of tetracycline by adsorption on biochar and pH has been observed in the literature [32,54–58] and is to be expected, since at low and high pH values the surface of the adsorbent and the tetracycline acquire charges of the same polarity, while the pH value leading to maximum removal varies, as the pHpzc values differ considerably. Activated biochar produced from sunflower seed husk [57] with a pHpzc of 4.4 achieves optimal removal of tetracycline at a pH between 5 and 7, closely resembling the properties and behaviour of BC-500 tested in this study.

Among the materials tested, BC-500 is particularly interesting because it is produced at a relatively low temperature without the use of chemical agents and therefore has the potential to become an economical and environmentally friendly adsorbent. Due to the lower pyrolysis temperature compared to the other adsorbents in this work, it is not unexpected that BC-500 has a lower specific surface area, but a higher content of surface functional groups that can interact with polar compounds [59] as revealed by BET and FTIR analysis (section 3.1). Considering this fact and the significantly higher number of proton acceptor (H_{acc}) and donor sites (H_{don}) as well as the polar surface area (*PSA*) of tetracycline compared to other tested molecules (Fig. S2e), we can hypothesise that hydrogen bonding and dipole-dipole interactions are the mechanisms responsible for adsorption.

Considering BC-800, based on the magnitude of the model coefficients shown in Eq. (3), the interaction between solid-to-liquid ratio and pH value had the largest effect on removal efficiency, while pH value had a slightly smaller effect and the interaction between pH and ionic strength had the smallest effect. Among the main effects, only pH was significant with a quadratic relationship to removal efficiency, as shown in Fig. S5. However, as the interactions are statistically significant, it would be inappropriate to discuss the main effect without considering the values of the other factors. The interactions are illustrated in Fig. 4. It can be seen from Fig. 4a that a lower pH requires a higher adsorbent dose and, conversely, a higher pH requires a lower adsorbent dose to achieve a higher tetracycline removal efficiency. Considering that ionic interactions are likely to be repulsive at high pH values since tetracycline has a negative charge, it could be that a lower solid-liquid ratio results in a lower total surface area whose negative charge can be neutralised by the given amount of KCl in solution, preventing electrostatic repulsion. On the contrary, at low pH values, where tetracycline has a positive charge, a higher solid-to-liquid ratio is required because the total surface area is larger and its charge cannot be neutralised by the available amount of KCl in the solution, thus allowing the attractive ionic interactions. The relationships shown in Fig. 4b and c at different values of ionic strength support this conclusion. Similar conclusions can be drawn from the interaction between the pH value of the solution and the ionic strength shown in Fig. 4d. In Ref. [60], the authors applied the Box-Behnken design to optimise the removal of Eriochrome Black T by the magnetic nanocomposite based on biochar. Ionic strength also showed a significant effect through the interaction with pH and it was also found that the effect of ionic strength can be positive or negative depending on whether

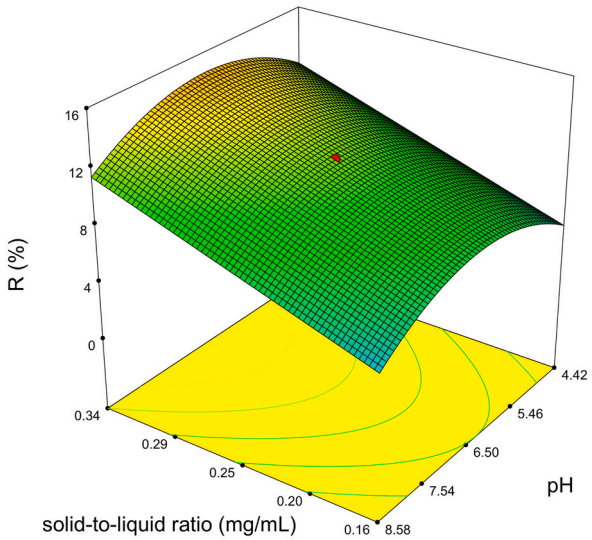

Fig. 3. Dependence of tetracycline removal efficiency of BC-500 on the solid-to-liquid ratio and pH of solution at the fixed ionic strength of 165 mM. The red dots correspond to the removal efficiency at the middle level of the factors. (For interpretation of the references to colour in this figure legend, the reader is referred to the Web version of this article.)

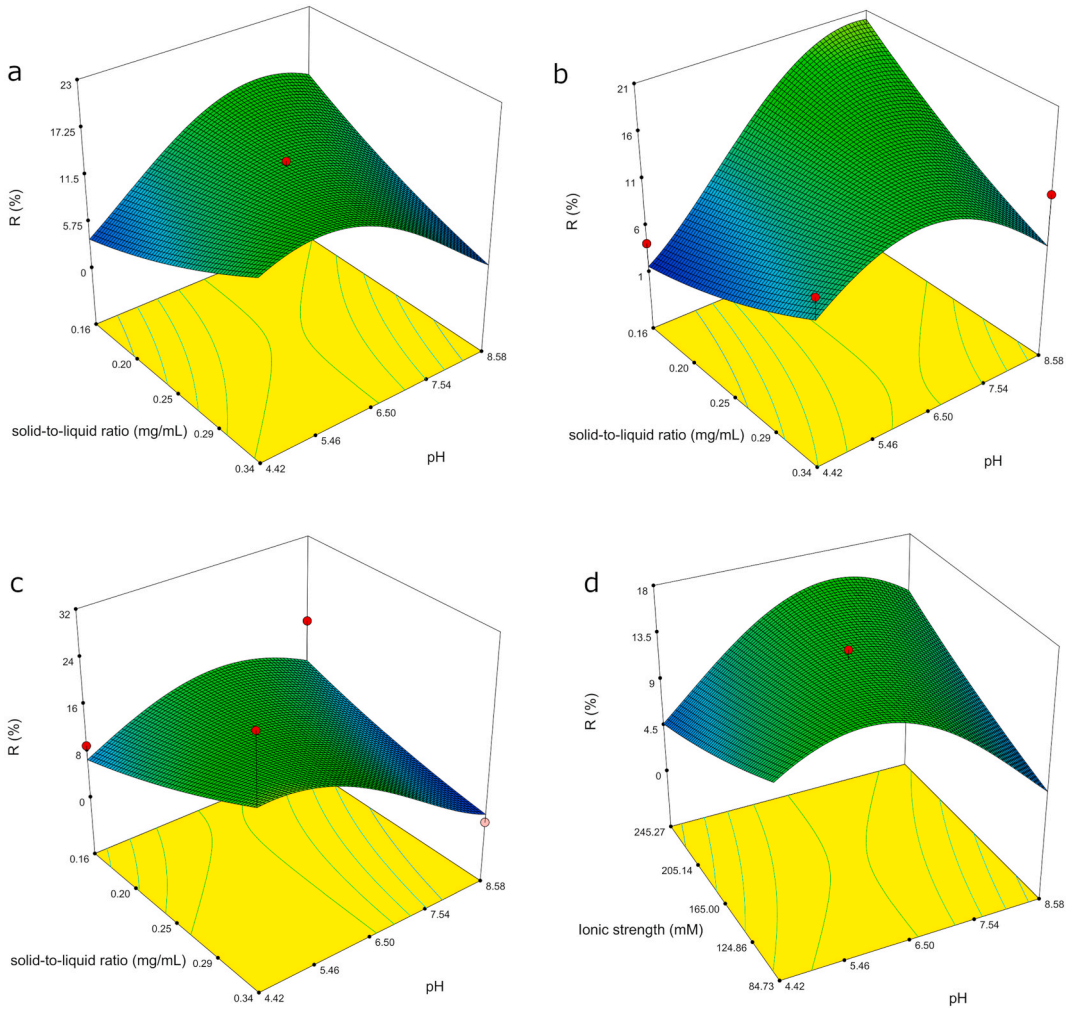

Fig. 4. Dependence of the tetracycline removal efficiency of BC-800 on experimental factors: pH and solid-to-liquid ratio at the different ionic strengths of the solution: a) 165 mM, b) 245.27 mM, c) 84.73 mM; d) pH and ionic strength of solution at the solid-to-liquid ratio of 0.25 mg mL^{-1}.

the pH favors attractive or repulsive electrostatic interactions. In the case of BC-800, the interactions between the factors that significantly influence the system would remain unrecognised in the OFAT approach.

Since tetracycline was the only substance adsorbed, its hydrogen bonding ability and polarity could also be the prerequisites for adsorption on BC-800. However, considering that BC-800 has a much smaller number of functional groups on the surface than BC-500 as expected due to the higher pyrolysis temperature [59] and indicated by FTIR analysis (Fig. 2), hydrogen bonding and dipole interactions are unlikely to be important for the adsorption of tetracycline on BC-800. As the pyrolysis temperature increases, the surface area typically increases up to 500–600 °C depending on the lignin content in the biomass and then starts to decrease due to the so-called thermal deactivation [61]. According to BET analysis, BC-800 has a lower surface area compared to BC-500, which is consistent with the trend reported in the literature. Therefore, it seems unlikely that dispersion forces are involved in the adsorption process.

Although BC-500 and BC-800 can be subject to further physicochemical characterissation to gain a deep mechanistic understanding of the adsorption process, the chemometrically-aided approach clearly shows the limited applicability of these materials due to the high selectivity for adsorbates with certain properties. In addition, the DoE study of the adsorption conditions shows that these adsorbents generally perform poorly over the entire experimental range investigated. Therefore, it seems more appropriate to perform a screening of other adsorbents using a chemometrically based approach until the most versatile solution to the adsorption problem of interest is found.

3.6. Adsorption of model substances on AcBC-800

In contrast to previously tested adsorbents, AcBC-800 was able to remove all tested model substances to a considerable extent. The models in the case of atenolol, paracetamol, ketorolac and tetracycline are represented by the following equations, respectively:

$$R(\%) = 24.94 + 10.30 \times A + 3.03 \times B \quad (5)$$

$$R(\%) = 38.31 + 13.02 \times A \quad (6)$$

$$R(\%) = 40.24 + 14.22 \times A - 2.59 \times B \quad (7)$$

$$R(\%) = 27.98 + 7.96 \times A - 2.28 \times B \quad (8)$$

In all the above models, A stands for the solid-to-liquid ratio and B for the pH of the solution. Since a higher removal is obtained by using AcBC-800 compared to the previously studied BCs, the obtained empirical models have a much better performance, as shown in Table S4. For comparison, the mean value of tetracycline removal efficiency was 28 %, which is significantly higher than for BC-500 and BC-800. Neither the ionic strength nor the interactions between the experimental factors studied were significant.

The high predicted R^2 values shown in Table S4 imply that the models can be used not only to identify the most influential factors but also to determine optimal conditions concerning the experimental factors studied. Since pyrolysis is carried out at 800 °C after impregnation with $ZnCl_2$, it is conceivable that the adsorbent prepared, i.e., AcBC-800, has a drastically larger surface area and more extensive pore network, as well as a higher content of functional groups than BC-800 [9]. This was confirmed by FTIR and BET analysis (Section 3.1). The high precision of the experiments repeated under the conditions of the central point of the CCD (see the red dots corresponding to the central point in Fig. 5) which can be attributed to the significantly increased specific surface area. Although surface heterogeneity may or may not be preserved by $ZnCl_2$ activation, the surface area is largely increased, suggesting that the amounts of AcBC-800 used in the adsorption tests are capable of representing the full chemical diversity of the surface. Therefore, the adsorption performances under identical test conditions with different adsorbent samples show significantly lower variations compared to non-activated biochars. While the increased specific surface area of the adsorbent led to high precision in the results of experiments replicated at the central point, the structural features of AcBC-800 allowed for a generally higher removal efficiency

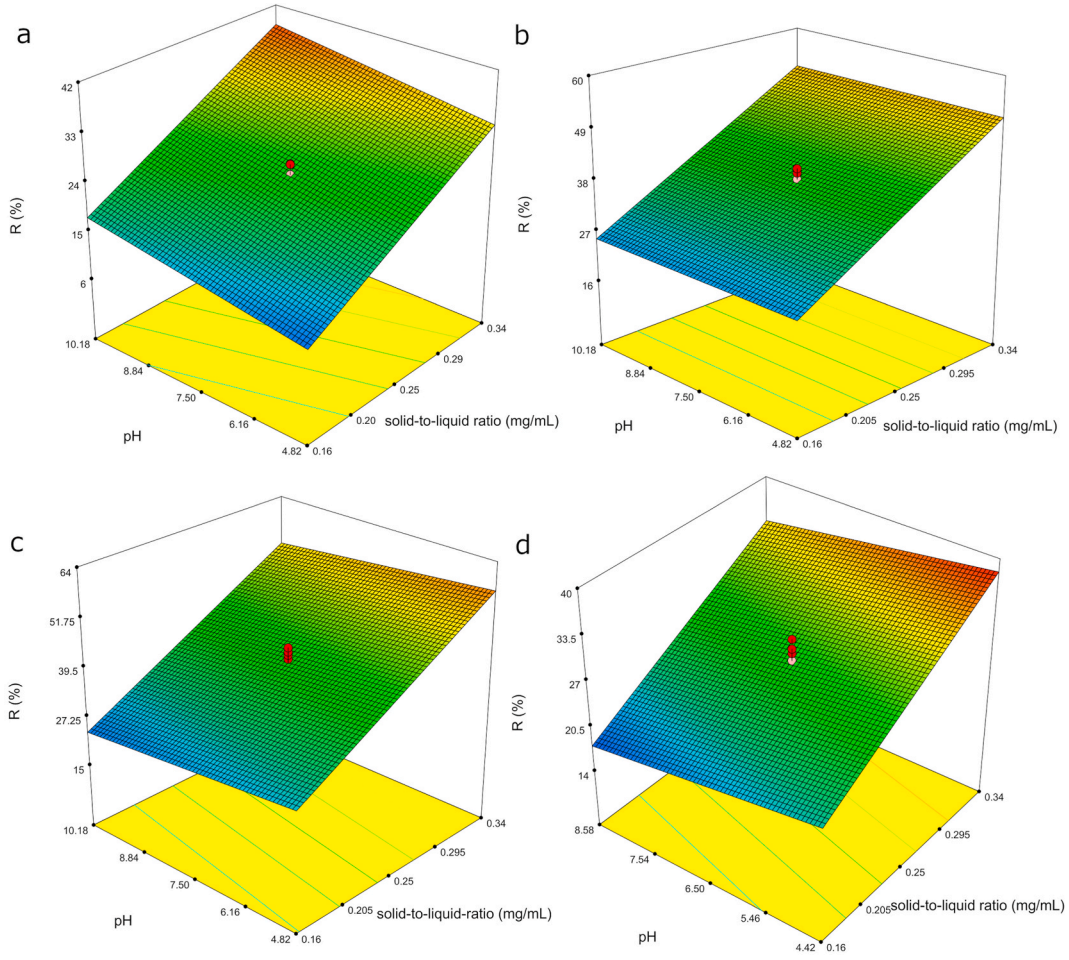

Fig. 5. Influence of solid-to-liquid ratio and pH at the fixed ionic strength level (165 mM) on: a) atenolol; b) paracetamol; c) ketorolac; d) tetracycline removal efficiency of AcBC-800.

compared to the previously tested BCs, and more pronounced changes were observed when the values of the investigated factors were changed. At the same time, these effects led to models with high prediction accuracy. In conjunction with previous findings, this emphasises the need for the response changes under varying experimental conditions to significantly exceed the experimental error. The fulfilment of this requirement depends on the inherent nature of the system. Consequently, it can be assumed that highly accurate predictive models may not be feasible for certain adsorption systems such as BC-500 or BC-800.

Fig. 5 and Fig. S6 shows that the effect of pH on removal efficiency was unique for each of the drug substances studied. The lack of a significant influence of pH on the adsorption of paracetamol (Fig. 5b) is to be expected, as paracetamol is mainly present in its molecular form and thus shows only minor variations in its molecular properties over the pH range studied. Moon et al., who investigated the adsorption of paracetamol on activated biochar from *Spirulina* sp., also observed no significant influence of the pH value in the range 2–9 [62]. Other studies have examined pH in extended ranges (2.5–12.5 and 2–14) and found a slight decrease in removal with increasing pH, which is due to ionisation of paracetamol at higher pH values and electrostatic repulsion with the negatively charged surface of the adsorbent [63,64]. The ranges investigated in this study were not sufficient to achieve a significant degree of paracetamol ionisation, which explains the insignificant effect of pH. With regard to the adsorption of atenolol, the increase in pH led to an increased removal efficiency (Fig. 5a and Fig. S6a). In the study of adsorption of pharmaceuticals on activated biochar from palm kernel shell [33] it was found that amount of atenolol adsorbed increases with increased pH, which was attributed to decreasing electrostatic repulsions. Another study on the adsorption of atenolol on biochar-montmorillonite composite discovered the initial increase in adsorption capacity with increasing pH, followed by a decrease as atenolol is deprotonated and no longer has a positive charge that can form ionic interactions with the negatively charged surface of the adsorbent [65]. On the contrary, it is unlikely that the adsorption of atenolol on AcBC-800 is dependent on ionic interactions, since lower pH values leading to a negatively charged surface of the adsorbent that coincides with positively charged atenolol do not lead to increased removal efficiency. Ketorolac, whose adsorption on biochar has not yet been studied in the literature, was most efficiently removed under conditions unfavourable to attractive ionic interactions (Fig. 5c and Fig. S6b). Moreover, the deviation from the generally observed quadratic relationship between removal efficiency and pH [32,54–58] in the case of tetracycline adsorption on AcBC-800 (Fig. S6c) is further evidence that ionic interactions do not make a significant contribution.

The solid-to-liquid ratio had a positive linear influence regardless of the drug molecule tested (Fig. 5 and Fig. S7), which is consistent with the results in the literature [55,66]. The magnitude of the model coefficients in Eqs. (5)–(8) and response surface plots in Fig. 5 indicate that the solid-to-liquid ratio had a more pronounced effect than pH in all the cases considered. However, it is important to emphasize that the removal efficiency of AcBC-800 was relatively high for all model substances tested over the entire investigated factors' ranges. Such robust performance favours the broad range of possible applications of AcBC-800, as pH adjustment may not be required to achieve the desired extent of adsorption in practice. The insignificance of the ionic strength in the studied range, i.e. the absence of a negative influence on the removal efficiency, may also be beneficial. Even a low dosage of adsorbent, such as 0.16 mg mL^{-1}, can result in a significant removal efficiency, allowing lower material consumption with sufficient performance in real-world applications. However, when characterising an adsorbent, the removal efficiency, i.e., the change in solute concentration due to adsorption, should be as high as possible compared to the experimental error to reliably describe the kinetics and equilibrium of the adsorption process. Therefore, a higher dose of the adsorbent is a favorable choice for further studies of the adsorption kinetics and equilibria.

In the case of adsorption of atenolol on AcBC-800, the pH value resulting in the highest removal efficiency was 10.18 as indicated by the response surface in Fig. 5a. However, this pH value leads to much lower solubility of atenolol and precipitation when the concentration of the solution is high (e.g. 200 μg mL^{-1}), i.e., in the study of adsorption equilibrium. In addition, the predominant form of atenolol at pH 10.18 is neutral (about 90 %), but there is still about 10 % of the cationic form, so the kinetics and equilibrium studies under such conditions would describe the adsorption of two molecular species that differ significantly in their properties and consequently in the mechanism of adsorption. To address this problem, a pH of 6.5 was defined as optimal for the adsorption of atenolol, ensuring that the cationic form was almost exclusively present and that the solubility of atenolol was suitable. The experimental conditions leading to optimal removal efficiency of the tested activated biochars, as determined by CCD, are listed in Table 1. The results of the experimental verification of the predicted optimal removal efficiencies are shown in Table S6. Table S6 shows that in the case of AcBC-800 all experimentally determined removal efficiencies lie within the 95 % prediction interval.

Due to the consistently negative zeta potential values (Fig. 1) across the entire pH range, it was expected that the adsorbent would have a greater affinity for adsorbates with positive charges (atenolol, tetracycline). However, contrary to expectations, these substances were removed less efficiently than neutral and anionic substances (paracetamol, ketorolac), suggesting that ionic interactions

Table 1
Optimal removal efficiencies, corresponding adsorbed amounts of the tested substances and the levels of the studied experimental factors leading to optimal removal efficiency of AcBC-650 and AcBC-800.

Adsorbent	Model substance	Solid-to-liquid ratio (mg mL^{-1})	pH	Ionic strength (mM KCl)	Removal efficiency (%)	Adsorbed amount (mg g^{-1})
AC 800	Atenolol	0.34	6.5	165	34.1	50.3
	Paracetamol		7.5		51.3	75.6
	Ketorolac		6.0		55.9	82.4
	Tetracycline		4.4		38.2	56.3
AC 650	Atenolol	0.34	6.5	245	23.4	34.3
	Ketorolac		6.0	165	41.8	61.4

Note: The adsorbed amount is calculated based on the remaining drug concentration after 60 min, i.e. it is not the equilibrium adsorption capacity.

probably play a minor role in the adsorption process.

Since all model substances were significantly adsorbed, the relationship between molecular properties and the degree of removal was acquired, so a correlation analysis was performed. The reason for selecting the adsorbed amount (q_t) as the dependent variable in this case is due to the fact that this response was less influenced by the solid-to-liquid ratio (SLR) compared to the removal efficiency, as can be seen in Fig. 6. When the removal efficiency and a single molecular descriptor are correlated, the high influence of SLR leads to a strong scattering of the response, resulting in low correlation coefficients (Fig. 6). In Fig. 6, the highest correlations of the adsorbed amount were with the number of proton donor sites (H_{don}) and the maximal projection radius (*MPR*), closely followed by *logD*. The van der Waals volume (*VdW* volume), polarizability, and polar surface area (*PSA*) showed lower correlations, while the lowest correlations were observed for dipole moment, total charge and the number of proton acceptor sites (H_{acc}). It is important to note that none of the correlations of q_t with individual molecular properties were outstanding compared to other correlations, likely indicating multiple mechanisms involved in drug adsorption on AcBC-800.

A positive correlation between q_t and *logD*, suggests the important role of hydrophobic interactions. The negative correlation of the observed response with *PSA* and dipole moment supports this hypothesis. The negative correlation between q_t and *MPR* suggests that molecular size plays a crucial role and exerts a negative influence on adsorption extent. Consequently, mechanisms such as pore filling and size exclusion are likely to have significant impacts. The highest negative correlation between q_t and H_{don} is quite unexpected. A higher H_{don} value may actually indicate a greater ability of the drug molecule to form hydrogen bonds with water molecules. The hydration of the molecules probably affects the distribution of the drug molecules in the adsorption system, so that the drug molecules are more likely to remain in the solution. Although H_{acc}, which represents the number of lone electron pairs on the electronegative atoms of a drug molecule, should have a similar effect on the hydration of a molecule as H_{don}, the correlation of removal efficiency with H_{acc} was considerably lower. Since the zeta potential of AcBC-800 is generally higher than that of non-modified BCs tested, it is possible that positively charged centers on the surface of AcBC-800, capable of forming ion-dipole and ionic interactions with the lone electron pairs of the drug molecules, were introduced by the activation. Another possibility is that some proton donors, which can form hydrogen bonds with proton acceptor sites of adsorbate molecules, are present on the surface of the adsorbent. Accordingly, it may be that the negative effect of H_{acc} on removal efficiency caused by the higher hydration ability of a molecule conflicts with the positive effect caused by attractive interactions with surface functional groups of AcBC-800. These opposing effects probably led to a negative but low correlation between q_t and H_{acc}.

Considering the significantly developed specific surface area (346.6 $m^2\ g^{-1}$) and the presence of hydroxyl groups on the surface of AcBC-800, as indicated by the FTIR spectra (Fig. 2), the above hypotheses about the adsorption mechanisms seem reasonable. As the number of drug substances tested was too small, the adsorption mechanisms indicated by the correlation analysis should not be generalised but considered as a hypothesis. However, the approach used shows that systematically changing the experimental conditions by DoE resulted in significant changes in molecular properties and therefore provided more data points for testing the

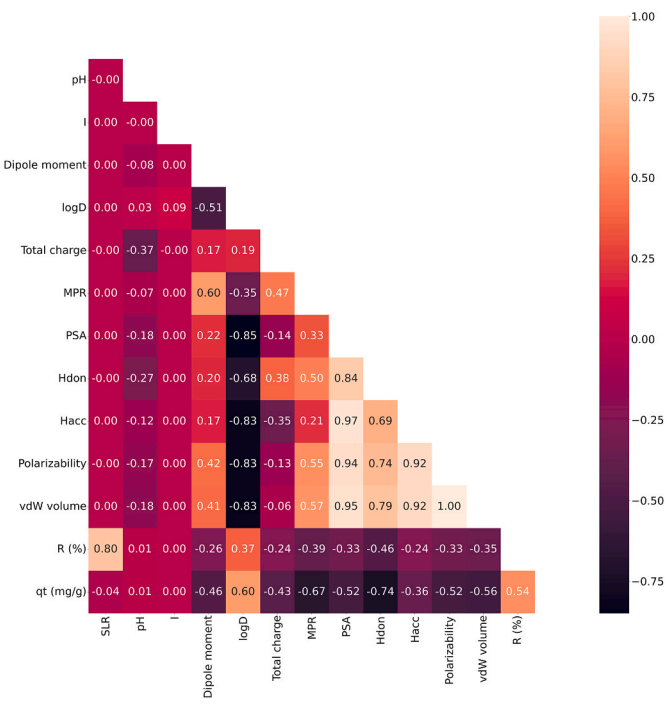

Fig. 6. Heatmap representing the correlations between all variables in a dataset (SLR stands for the solid-to-liquid ratio, and MPR for the maximal projection radius).

correlations between removal efficiency and molecular properties. This strategy could be used for a more comprehensive study in which relationships between the molecular properties of a large number of drugs and their adsorption behavior should be established to draw general conclusions regarding the mechanism of drug adsorption on an optimal adsorbent.

3.7. Adsorption of model substances on AcBC-650

In the concluding phase of adsorbent comparison and selection, we sought to investigate whether activation at lower temperatures could produce a material capable of effectively binding drug molecules. Although a lower activation temperature can lead to a lower specific surface area and a lower micro- and mesopore volume, it can be advantageous as it allows a higher yield of AcBC, a higher content of heteroatoms and lower energy consumption [67]. To achieve our goal without the extensive consumption of activated carbon prepared at 650 °C (AcBC-650), which was only available in limited quantities, we investigated the adsorption of only two drugs – atenolol and ketorolac. Of the model compounds studied, atenolol showed the lowest adsorption, while ketorolac showed the highest adsorption on AcBC-800. The results obtained therefore not only allow a quantitative comparison of adsorption on AcBC-650 and AcBC-800 but also provide insight into the possible differences in the selectivity of the materials tested. The differences in the selectivity of these materials for the model adsorbates could be due to the different pyrolysis temperatures, which may affect the abundance of surface functional groups and the efficiency of pore development.

The application of the CCD to study the adsorption of atenolol and ketorolac on AcBC-650 has led to the following models, respectively:

$$R\,(\%) = 15.81 + 6.65 \times A + 0.90 \times C \tag{9}$$

$$R\,(\%) = 28.69 + 10.28 \times A - 4.97 \times B \tag{10}$$

The terms A, B and C represent the solid-to-liquid ratio, the pH and the ionic strength of the solution respectively. Similar to AcBC-800, the high adjusted and predicted R^2 values (Table S4) and the close agreement of the removal efficiencies obtained by replicating the experiments in the central point of the CCD is probably due to the significantly increased specific surface area (93.4 $m^2\ g^{-1}$) compared to non-activated BCs as explained for AcBC-800.

The extent of removal of atenolol and ketorolac under optimal conditions is shown in Table 1. AcBC-650 exhibited a greater affinity for ketorolac compared to atenolol, as evidenced by a higher removal efficiency under optimal conditions. The dissimilarity in lipophilicity between atenolol and ketorolac suggests that the difference in removal efficiency can be ascribed to a hydrophobic effect. The fact that AcBC-650 similarly adsorbs the model substances to AcBC-800 implies that the underlying adsorption mechanisms are not markedly different. Nonspecific interactions, including van der Waals forces and the hydrophobic effect, are likely governing the adsorption process. The lower removal of atenolol and ketorolac relative to AcBC-800 can be attributed to the considerably lower specific surface area of AcBC-650 resulting from a lower activation temperature.

Comparing the values of coefficients in the models shown in Eq. (9) and Eq. (10), it can be seen that the ratio of solid to liquid was the most influential factor in both cases. Adsorption of atenolol on AcBC-650 showed that increased solid-to-liquid ratio and higher ionic strength in the solution were associated with improved removal efficiency (Fig. S8). The positive effect of ionic strength on removal efficiency throughout the pH range tested (Fig. S8b) probably results from the "salting out" effect that favors the water-solid distribution of solutes towards the solid, i.e. adsorbed phase. It is interesting to note that the pH of the solution had no significant effect. This could indicate that the *logD* values of atenolol are too low over the entire pH range, therefore pH-driven changes in the hydrophobic effect are not significant. Since the pH value has no significant influence, the surface charge of AcBC-650 appears to have a negligible effect on the adsorption of atenolol.

The solid-to-liquid ratio also has a positive linear effect on the degree of removal of ketorolac (Fig. S9a). From the negative sign of the model coefficient B and main effect plot shown in Fig. S9b, it can be concluded that the efficiency of ketorolac removal by AcBC-650 decreases with increasing pH, which could be due to the increasing negative charge of the surface of AcBC-650 (Fig. 1) and the strong repulsion with the anionic form of ketorolac. Lower pH values are associated with higher *logD* values, possibly leading to higher adsorption through hydrophobic interactions. The effect of ionic strength was not significant, which may indicate that for the substances with relatively high *logD* values, the changes in hydrophobic effect due to the change in ionic strength of the solution are negligible.

By selecting model substances with the highest and lowest affinity for AcBC-800 as adsorbates for the study of AcBC-650, it was possible to obtain an indication of possible changes in the selectivity of the adsorbent. However, in our case, AcBC-650 and AcBC-800 both showed a higher affinity for ketorolac compared to atenolol, so it can be assumed that the adsorption of AcBC-650 and AcBC-800 is determined by the similar types of interactions and there is no significant difference in selectivity of tested adsorbents. Since the extent of removal of both model compounds by AcBC-650 was lower compared to AcBC-800, it can be assumed that AcBC-650 generally has a lower drug removal efficiency, which positions this adsorbent as a less efficient alternative.

4. Conclusions

In this study, the leaf of *A. altissima* proves to be a suitable starting material for the preparation of carbonaceous adsorbents. The production of activated biochar from *A. altissima* can expand the range of available low-cost and environmentally friendly adsorbents, offer the possibility of using an invasive plant and thus contribute to the sustainability of adsorption processes and environmental management. Among the materials tested, AcBC-800 achieved the highest removal efficiency of atenolol, tetracycline, paracetamol

and ketorolac, and was therefore selected for further testing. This confirms that impregnation with $ZnCl_2$ and carbonization at high temperatures effectively transforms the leaves of *A. altissima* into a highly efficient drug adsorbent. The FTIR spectra revealed that increasing the pyrolysis temperature without the $ZnCl_2$ activating agent decreases the intensity of all bands. However, the activation helps preserve the functional groups, as evidenced by the spectra of biochars pyrolysed at 650 and 800 °C. Additionally, high temperatures during activation promoted the development of an efficient surface area, with the maximum observed for AcBC-800 reaching 347 $m^2 g^{-1}$. CCD was successfully applied to determine the experimental conditions that lead to optimal removal efficiency and under which further adsorption studies and comparisons of adsorbents should be conducted. The investigation of BC-500 and BC-800 has shown that the predictive ability of DoE models can be limited by the low removal efficiency compared to the experimental variability. The careful selection of drug model substances together with the systematic variation of the experimental conditions by the DoE along with the characterisation of adsorbents allowed some mechanistic insights into the adsorption systems investigated. Nevertheless, the results obtained in this study regarding adsorption mechanisms should not be generalised as the number of drug model compounds is small. Instead, this study represents the starting point for extensive testing of the most suitable adsorbent with diverse subgroups of drugs. Furthermore, the presented case study is an example of a chemometrically-aided approach that can serve as a framework for conducting a reliable and efficient adsorbent screening before investigating the novel adsorptive materials in detail.

Funding

This work was supported by the Ministry of Education, Science and Technological Development, Republic of Serbia through Grant Agreements with University of Belgrade – Faculty of Pharmacy [grant number 451-03-66/2024-03/200161 and 451-03-65/2024-03/200161], with Institute of Technology of Nuclear and Other Mineral Row Materials - ITNMS, Belgrade [grant number 451-03-66/2024-03/200023] and with University of Belgrade – Faculty of Physical Chemistry [grant number 451-03-65/2024-03/200146].

Data availability statement

The data for this study are contained in the article and in the supplementary material.

CRediT authorship contribution statement

Jevrem Stojanović: Writing – original draft, Investigation, Formal analysis. **Maja Milojević-Rakić:** Writing – review & editing, Formal analysis. **Danica Bajuk-Bogdanović:** Investigation, Writing – review & editing. **Dragana Ranđelović:** Writing – review & editing, Resources, Investigation. **Miroslav Sokić:** Writing – review & editing, Formal analysis, Funding acquisition. **Biljana Otašević:** Writing – review & editing, Methodology. **Anđelija Malenović:** Writing – review & editing, Methodology, Conceptualization. **Aleksandra Janošević Ležaić:** Writing – review & editing, Supervision, Conceptualization, Project administration. **Ana Protić:** Writing – review & editing, Supervision, Conceptualization, Project administration.

Declaration of competing interest

The authors declare that they have no known competing financial interests or personal relationships that could have appeared to influence the work reported in this paper.

Appendix A. Supplementary data

Supplementary data to this article can be found online at https://doi.org/10.1016/j.heliyon.2024.e34841.

References

[1] K. Weber, P. Quicker, Properties of biochar, Fuel 217 (2018) 240–261, https://doi.org/10.1016/j.fuel.2017.12.054.
[2] J.S. Cha, S.H. Park, S.-C. Jung, C. Ryu, J.-K. Jeon, M.-C. Shin, Y.-K. Park, Production and utilization of biochar: a review, J. Ind. Eng. Chem. 40 (2016) 1–15, https://doi.org/10.1016/j.jiec.2016.06.002.
[3] N.L. Panwar, A. Pawar, Influence of activation conditions on the physicochemical properties of activated biochar: a review, Biomass Conversion and Biorefinery 12 (2022) 925–947, https://doi.org/10.1007/s13399-020-00870-3.
[4] R. He, X. Yuan, Z. Huang, H. Wang, L. Jiang, J. Huang, M. Tan, H. Li, Activated biochar with iron-loading and its application in removing Cr (VI) from aqueous solution, Colloids Surf. A Physicochem. Eng. Asp. 579 (2019) 123642, https://doi.org/10.1016/j.colsurfa.2019.123642.
[5] C. Kalinke, P.R. Oliveira, G.A. Oliveira, A.S. Mangrich, L.H. Marcolino-Junior, M.F. Bergamini, Activated biochar: preparation, characterization and electroanalytical application in an alternative strategy of nickel determination, Anal. Chim. Acta 983 (2017) 103–111, https://doi.org/10.1016/j.aca.2017.06.025.
[6] K.A. Thompson, K.K. Shimabuku, J.P. Kearns, D.R.U. Knappe, R.S. Summers, S.M. Cook, Environmental comparison of biochar and activated carbon for tertiary wastewater treatment, Environ. Sci. Technol. 50 (2016) 11253–11262, https://doi.org/10.1021/acs.est.6b03239.
[7] K.Y. Foo, B.H. Hameed, Insights into the modeling of adsorption isotherm systems, Chem. Eng. J. 156 (2010) 2–10, https://doi.org/10.1016/j.cej.2009.09.013.
[8] F. Maya, C. Palomino Cabello, M. Ghani, G. Turnes Palomino, V. Cerdà, Emerging materials for sample preparation, J. Separ. Sci. 41 (2018) 262–287, https://doi.org/10.1002/jssc.201700836.

[9] D.C.C.daS. Medeiros, C. Nzediegwu, C. Benally, S.A. Messele, J.-H. Kwak, M.A. Naeth, Y.S. Ok, S.X. Chang, M. Gamal El-Din, Pristine and engineered biochar for the removal of contaminants co-existing in several types of industrial wastewaters: a critical review, Sci. Total Environ 809 (2022) 151120, https://doi.org/10.1016/j.scitotenv.2021.151120.

[10] J.A. Ippolito, L. Cui, C. Kammann, N. Wrage-Mönnig, J.M. Estavillo, T. Fuertes-Mendizabal, M.L. Cayuela, G. Sigua, J. Novak, K. Spokas, N. Borchard, Feedstock choice, pyrolysis temperature and type influence biochar characteristics: a comprehensive meta-data analysis review, Biochar 2 (2020) 421–438, https://doi.org/10.1007/s42773-020-00067-x.

[11] C. Enescu, T. Durrant, G. Caudullo, Ailanthus Altissima in Europe: Distribution, Habitat, Usage and Threats, 2016.

[12] I. Kowarik, I. Säumel, Biological flora of central europe: Ailanthus altissima (mill.) swingle, perspectives in plant ecology, Evolution and Systematics 8 (2007) 207–237, https://doi.org/10.1016/j.ppees.2007.03.002.

[13] I. Ihsanullah, M.T. Khan, M. Zubair, M. Bilal, M. Sajid, Removal of pharmaceuticals from water using sewage sludge-derived biochar: a review, Chemosphere 289 (2022) 133196, https://doi.org/10.1016/j.chemosphere.2021.133196.

[14] L.L.A. Melo, A.H. Ide, J.L.S. Duarte, C.L.P.S. Zanta, L.M.T.M. Oliveira, W.R.O. Pimentel, L. Meili, Caffeine removal using Elaeis guineensis activated carbon: adsorption and RSM studies, Environ. Sci. Pollut. Control Ser. 27 (2020) 27048–27060, https://doi.org/10.1007/s11356-020-09053-z.

[15] S. Mondal, K. Aikat, K. Siddharth, K. Sarkar, R. DasChaudhury, G. Mandal, G. Halder, Optimizing ranitidine hydrochloride uptake of Parthenium hysterophorus derived N-biochar through response surface methodology and artificial neural network, Process Saf. Environ. Protect. 107 (2017) 388–401, https://doi.org/10.1016/j.psep.2017.03.011.

[16] R. Tremea, H.B. Quesada, R. Bergamasco, F. Bassetti, J. de, Influence of important parameters on the adsorption of diclofenac sodium by an environmentally friendly eucalyptus wood biochar and optimization using response surface methodology, Desalination Water Treat 230 (2021) 384–399. https://doi.org/10.5004/dwt.2021.27411.

[17] A.J. Siddiqui, N. Kumari, M. Adnan, S. Kumar, A. Abdelgadir, J. Saxena, R. Badraoui, M. Snoussi, P. Khare, R. Singh, Impregnation of modified magnetic nanoparticles on low-cost agro-waste-derived biochar for enhanced removal of pharmaceutically active compounds: performance evaluation and optimization using response surface methodology, Water 15 (2023), https://doi.org/10.3390/w15091688.

[18] C. Ebere Enyoh, Q. Wang, S. Lu, Optimizing the efficient removal of ciprofloxacin from aqueous solutions by polyethylene terephthalate microplastics using multivariate statistical approach, Chem. Eng. Sci. 278 (2023) 118917, https://doi.org/10.1016/j.ces.2023.118917.

[19] J. Stojanović, J. Krmar, A. Protić, B. Svrkota, N. Đajić, B. Otašević, Experimental design in HPLC separation of pharmaceuticals, Arhiv Za Farmaciju 71 (2021) 279–301, https://doi.org/10.5937/arhfarm71-32480.

[20] G.S. dos Reis, S.H. Larsson, M. Mathieu, M. Thyrel, T.N. Pham, Application of design of experiments (DoE) for optimised production of micro- and mesoporous Norway spruce bark activated carbons, Biomass Conversion and Biorefinery 13 (2023) 10113–10131, https://doi.org/10.1007/s13399-021-01917-9.

[21] M.C. Ndoun, H.A. Elliott, H.E. Preisendanz, C.F. Williams, A. Knopf, J.E. Watson, Adsorption of pharmaceuticals from aqueous solutions using biochar derived from cotton gin waste and guayule bagasse, Biochar 3 (2021) 89–104, https://doi.org/10.1007/s42773-020-00070-2.

[22] A. Maged, P.D. Dissanayake, X. Yang, C. Pathirannahalage, A. Bhatnagar, Y.S. Ok, New mechanistic insight into rapid adsorption of pharmaceuticals from water utilizing activated biochar, Environ. Res. 202 (2021) 111693, https://doi.org/10.1016/j.envres.2021.111693.

[23] Y. Zhou, X. Liu, Y. Xiang, P. Wang, J. Zhang, F. Zhang, J. Wei, L. Luo, M. Lei, L. Tang, Modification of biochar derived from sawdust and its application in removal of tetracycline and copper from aqueous solution: adsorption mechanism and modelling, Bioresour. Technol. 245 (2017) 266–273, https://doi.org/10.1016/j.biortech.2017.08.178.

[24] H.N. Tran, F. Tomul, N. Thi Hoang Ha, D.T. Nguyen, E.C. Lima, G.T. Le, C.-T. Chang, V. Masindi, S.H. Woo, Innovative spherical biochar for pharmaceutical removal from water: insight into adsorption mechanism, J. Hazard Mater. 394 (2020) 122255, https://doi.org/10.1016/j.jhazmat.2020.122255.

[25] C.M. Grisales-Cifuentes, E.A. Serna Galvis, J. Porras, E. Flórez, R.A. Torres-Palma, N. Acelas, Kinetics, isotherms, effect of structure, and computational analysis during the removal of three representative pharmaceuticals from water by adsorption using a biochar obtained from oil palm fiber, Bioresour. Technol. 326 (2021) 124753, https://doi.org/10.1016/j.biortech.2021.124753.

[26] R. Luo, X. Li, H. Xu, Y. Sun, J. Wu, Effects of temperature, solution pH, and ball-milling modification on the adsorption of non-steroidal anti-inflammatory drugs onto biochar, Bull. Environ. Contam. Toxicol. 105 (2020) 422–427, https://doi.org/10.1007/s00128-020-02948-0.

[27] S.-Y. Oh, Y.-D. Seo, Sorption of halogenated phenols and pharmaceuticals to biochar: affecting factors and mechanisms, Environ. Sci. Pollut. Control Ser. 23 (2016) 951–961, https://doi.org/10.1007/s11356-015-4201-8.

[28] R. Leardi, Chapter 2 - experimental design, in: F. Marini (Ed.), Data Handling in Science and Technology, Elsevier, 2013, pp. 9–53, https://doi.org/10.1016/B978-0-444-59528-7.00002-8.

[29] R. Leardi, Experimental design in chemistry: a tutorial, Anal. Chim. Acta 652 (2009) 161–172, https://doi.org/10.1016/j.aca.2009.06.015.

[30] Í.N. Raupp, A. Valério Filho, A.L. Arim, A.R. Muniz, G.S. da Rosa, Development and characterization of activated carbon from olive pomace: experimental design, kinetic and equilibrium studies in nimesulide adsorption, Materials 14 (2021), https://doi.org/10.3390/ma14226820.

[31] M. El-Azazy, I. Nabil, S.S. Hassan, A.S. El-Shafie, Adsorption characteristics of pristine and magnetic olive stones biochar with respect to clofazimine, Nanomaterials 11 (2021), https://doi.org/10.3390/nano11040963.

[32] H.M. Jang, S. Yoo, Y.-K. Choi, S. Park, E. Kan, Adsorption isotherm, kinetic modeling and mechanism of tetracycline on *Pinus taeda*-derived activated biochar, Bioresour. Technol. 259 (2018) 24–31, https://doi.org/10.1016/j.biortech.2018.03.013.

[33] M.-H. To, P. Hadi, C.-W. Hui, C.S.K. Lin, G. McKay, Mechanistic study of atenolol, acebutolol and carbamazepine adsorption on waste biomass derived activated carbon, J. Mol. Liq. 241 (2017) 386–398, https://doi.org/10.1016/j.molliq.2017.05.037.

[34] Y. Li, Z. Xu, Q. Zhang, J. Di, R. Yang, X. Gai, H. Wang, T. Zhang, Mesoporous biochar derived from bamboo waste: template/hydrothermal preparation and highly efficient pharmaceutical adsorption, Bioresources 18 (2023) 1882–1900, https://doi.org/10.15376/biores.18.1.1882-1900.

[35] S.L.C. Ferreira, R.E. Bruns, E.G.P. da Silva, W.N.L. dos Santos, C.M. Quintella, J.M. David, J.B. de Andrade, M.C. Breitkreitz, I.C.S.F. Jardim, B.B. Neto, Statistical designs and response surface techniques for the optimization of chromatographic systems, J. Chromatogr. A 1158 (2007) 2–14, https://doi.org/10.1016/j.chroma.2007.03.051.

[36] D.C. Montgomery, Design and Analysis of Experiments, John Wiley & Sons, 2008. https://books.google.rs/books?id=kMMJAm5bD34C.

[37] S.K. Milonjić, A.L. Ruvarac, M.V. Šušić, The heat of immersion of natural magnetite in aqueous solutions, Thermochim. Acta 11 (1975) 261–266, https://doi.org/10.1016/0040-6031(75)85095-7.

[38] J.-H. Yuan, R.-K. Xu, The amelioration effects of low temperature biochar generated from nine crop residues on an acidic Ultisol, Soil Use Manag. 27 (2011) 110–115, https://doi.org/10.1111/j.1475-2743.2010.00317.x.

[39] P.M. Sanka, M.J. Rwiza, K.M. Mtei, Removal of selected heavy metal ions from industrial wastewater using rice and corn husk biochar, Water, Air, Soil Pollut. 231 (2020) 244, https://doi.org/10.1007/s11270-020-04624-9.

[40] R.F. Pinheiro, A. Grimm, M.L.S. Oliveira, J. Vieillard, L.F.O. Silva, I.A.S. De Brum, É.C. Lima, Mu Naushad, L. Sellaoui, G.L. Dotto, G.S. dos Reis, Adsorptive behavior of the rare earth elements Ce and La on a soybean pod derived activated carbon: application in synthetic solutions, real leachate and mechanistic insights by statistical physics modeling, Chem. Eng. J. 471 (2023) 144484, https://doi.org/10.1016/j.cej.2023.144484.

[41] A. Grimm, G.S. dos Reis, V.M. Dinh, S.H. Larsson, J.-P. Mikkola, E.C. Lima, S. Xiong, Hardwood spent mushroom substrate–based activated biochar as a sustainable bioresource for removal of emerging pollutants from wastewater, Biomass Conversion and Biorefinery 14 (2024) 2293–2309, https://doi.org/10.1007/s13399-022-02618-7.

[42] M.R. Axet, O. Dechy-Cabaret, J. Durand, M. Gouygou, P. Serp, Coordination chemistry on carbon surfaces, Coord. Chem. Rev. 308 (2016) 236–345, https://doi.org/10.1016/j.ccr.2015.06.005.

[43] B.C. Smith, Infrared Spectral Interpretation: A Systematic Approach, CRC Press, 2018. https://books.google.rs/books?id=XoP5vgEACAAJ.

[44] Z. Jovanovic, D. Bajuk-Bogdanović, S. Jovanović, Ž. Mravik, J. Kovač, I. Holclajtner-Antunović, M. Vujković, The role of surface chemistry in the charge storage properties of graphene oxide, Electrochim. Acta 258 (2017) 1228–1243, https://doi.org/10.1016/j.electacta.2017.11.178.

[45] R. Wahab, S.G. Ansari, Y.S. Kim, M.A. Dar, H.-S. Shin, Synthesis and characterization of hydrozincite and its conversion into zinc oxide nanoparticles, J. Alloys Compd. 461 (2008) 66–71, https://doi.org/10.1016/j.jallcom.2007.07.029.
[46] Miguel Galván-Ruiz, Hernández Juan, Baños Leticia, Noriega-Montes Joaquín, Mario E. Rodríguez-García, Characterization of calcium carbonate, calcium oxide, and calcium hydroxide as starting point to the improvement of lime for their use in construction, J. Mater. Civ. Eng. 21 (2009) 694–698.
[47] Y.S. Al-Degs, M.I. El-Barghouthi, A.H. El-Sheikh, G.M. Walker, Effect of solution pH, ionic strength, and temperature on adsorption behavior of reactive dyes on activated carbon, Dyes Pigments 77 (2008) 16–23, https://doi.org/10.1016/j.dyepig.2007.03.001.
[48] F. Reguyal, A.K. Sarmah, Adsorption of sulfamethoxazole by magnetic biochar: effects of pH, ionic strength, natural organic matter and 17α-ethinylestradiol, Sci. Total Environ. 628–629 (2018) 722–730, https://doi.org/10.1016/j.scitotenv.2018.01.323.
[49] N. Cherkasov, Liquid-phase adsorption: common problems and how we could do better, J. Mol. Liq. 301 (2020) 112378, https://doi.org/10.1016/j.molliq.2019.112378.
[50] L. Jia, P. Cheng, Y. Yu, S. Chen, C. Wang, L. He, H. Nie, J. Wang, J. Zhang, B. Fan, Y. Jin, Regeneration mechanism of a novel high-performance biochar mercury adsorbent directionally modified by multimetal multilayer loading, J. Environ. Manag. 326 (2023) 116790, https://doi.org/10.1016/j.jenvman.2022.116790.
[51] E. Worch, Adsorption Technology in water treatment: fundamentals, processes, and modeling, in: Adsorption Technology in Water Treatment, De Gruyter, 2012, https://doi.org/10.1515/9783110240238.
[52] S. Mompelat, A. Jaffrezic, E. Jardé, B. Le Bot, Storage of natural water samples and preservation techniques for pharmaceutical quantification, Talanta 109 (2013) 31–45, https://doi.org/10.1016/j.talanta.2013.01.042.
[53] K.V. Kumar, S. Gadipelli, B. Wood, K.A. Ramisetty, A.A. Stewart, C.A. Howard, D.J.L. Brett, F. Rodriguez-Reinoso, Characterization of the adsorption site energies and heterogeneous surfaces of porous materials, J. Mater. Chem. A 7 (2019) 10104–10137, https://doi.org/10.1039/C9TA00287A.
[54] J. Dai, X. Meng, Y. Zhang, Y. Huang, Effects of modification and magnetization of rice straw derived biochar on adsorption of tetracycline from water, Bioresour. Technol. 311 (2020) 123455, https://doi.org/10.1016/j.biortech.2020.123455.
[55] Y. Dai, J. Li, D. Shan, Adsorption of tetracycline in aqueous solution by biochar derived from waste *Auricularia auricula* dregs, Chemosphere 238 (2020) 124432, https://doi.org/10.1016/j.chemosphere.2019.124432.
[56] H.M. Jang, E. Kan, Engineered biochar from agricultural waste for removal of tetracycline in water, Bioresour. Technol. 284 (2019) 437–447, https://doi.org/10.1016/j.biortech.2019.03.131.
[57] T.-B. Nguyen, T.-K.-T. Nguyen, W.-H. Chen, C.-W. Chen, X.-T. Bui, A.K. Patel, C.-D. Dong, Hydrothermal and pyrolytic conversion of sunflower seed husk into novel porous biochar for efficient adsorption of tetracycline, Bioresour. Technol. 373 (2023) 128711, https://doi.org/10.1016/j.biortech.2023.128711.
[58] B. Huang, D. Huang, Q. Zheng, C. Yan, J. Feng, H. Gao, H. Fu, Y. Liao, Enhanced adsorption capacity of tetracycline on porous graphitic biochar with an ultra-large surface area, RSC Adv. 13 (2023) 10397–10407, https://doi.org/10.1039/D3RA00745F.
[59] H. Khurshid, M.R.U. Mustafa, M.H. Isa, A comprehensive insight on adsorption of polyaromatic hydrocarbons, chemical oxygen demand, pharmaceuticals, and chemical dyes in wastewaters using biowaste carbonaceous adsorbents, Adsorpt. Sci. Technol. 2022 (2022) 9410266, https://doi.org/10.1155/2022/9410266.
[60] A.A. Akbarnezhad, F. Safa, Biochar-based magnetic nanocomposite for dye removal from aqueous solutions: response surface modeling and kinetic study, Russ. J. Appl. Chem. 91 (2018) 1856–1866, https://doi.org/10.1134/S1070427218110174.
[61] L. Leng, Q. Xiong, L. Yang, H. Li, Y. Zhou, W. Zhang, S. Jiang, H. Li, H. Huang, An overview on engineering the surface area and porosity of biochar, Sci. Total Environ. 763 (2021) 144204, https://doi.org/10.1016/j.scitotenv.2020.144204.
[62] S. Moon, Y.-J. Lee, S.-J. Park, C.-G. Lee, Enhanced removal of micropollutants from water using ZnCl2-modified Spirulina sp.-based biochar, J. Appl. Phycol. 36 (2024) 167–179, https://doi.org/10.1007/s10811-023-03122-9.
[63] M. Romdhani, A. Attia, C. Charcosset, S. Mahouche-Chergui, A. Ates, J. Duplay, R. Ben Amar, Optimization of paracetamol and chloramphenicol removal by novel activated carbon derived from sawdust using response surface methodology, Sustainability 15 (2023), https://doi.org/10.3390/su15032516.
[64] A. Solmaz, Z.A. Sari, M. Karta, T. Turna, A. Yücel, T. Depci, Production and characterization of activated carbon from pomegranate peel for pharmaceutical waste (paracetamol) removal: response surface methodology application, Water, Air, Soil Pollut. 234 (2023) 645, https://doi.org/10.1007/s11270-023-06641-w.
[65] C. Fu, H. Zhang, M. Xia, W. Lei, F. Wang, The single/co-adsorption characteristics and microscopic adsorption mechanism of biochar-montmorillonite composite adsorbent for pharmaceutical emerging organic contaminant atenolol and lead ions, Ecotoxicol. Environ. Saf. 187 (2020) 109763, https://doi.org/10.1016/j.ecoenv.2019.109763.
[66] MdA. Islam, M.K. Nazal, A.A. Akinpelu, M. Sajid, N.A. Alhussain, M. Ilyas, High performance adsorptive removal of emerging contaminant paracetamol using a sustainable biobased mesoporous activated carbon prepared from palm leaves waste, J. Anal. Appl. Pyrol. 180 (2024) 106546, https://doi.org/10.1016/j.jaap.2024.106546.
[67] D. Angın, E. Altintig, T.E. Köse, Influence of process parameters on the surface and chemical properties of activated carbon obtained from biochar by chemical activation, Bioresour. Technol. 148 (2013) 542–549, https://doi.org/10.1016/j.biortech.2013.08.164.